ERDC/CHL CHETN-IX-6
December 2001

US Army Corps of Engineers®

Modeling Navigation Conditions at Lock Approaches

by Richard L. Stockstill

INTRODUCTION: The lock approach research required the development of a method to rapidly evaluate the navigation conditions in lock approaches for various guard wall configurations. The idea was to numerically model many guard wall configurations and then evaluate the most promising designs in the physical model. The method was to select a numerical modeling technique and then evaluate the appropriateness of the model's use (validate) with comparisons to laboratory data. If the model adequately simulated the flow field produced by a guard wall, then various designs would be modeled in an attempt to gain general insight into the controlling features of guard walls. These simulation results could then be used to develop design ideas for further testing in the physical model.

MODEL CONSIDERATIONS: The choice of modeling method is important. The geometry of the guard wall dictates the flow patterns in the lock approach. Therefore, the numerical flow model had to be designed so that only the geometrical parameters of the wall were changed from design to design and that the model would not rely on empirical coefficients. Empirical rules such as head-discharge relations rely on coefficients that can be dependent on the flow. For example, the discharge coefficient is sensitive to the direction of the flow relative to the control structure. Rather, a model was needed that relied on a physical description of the design to compute the flow passing under the guard wall.

The next consideration was the dimensionality of the model. Obviously, a one-dimensional description would not provide the lateral variability of the flow and so would not provide a means of estimating outdraft or draw toward the guard wall. A two-dimensional (2-D, depth-averaged) model would provide the lateral variations, but would have difficulty simulating flow under the guard wall. A three-dimensional (3-D) model provides the best resolution of the physics; however, it was found too computationally intense to make production runs of numerous wall designs. The three-dimensional model required too much time in generating the 3-D computational mesh and too much high-performance computer resources to be a viable means of evaluating a large number of design alternatives.

A compromise was reached wherein a 2-D (depth-averaged) model was used with the lock wall being represented by a pressure field on the water surface. This simulated a surface pressure head at the wall location equal to the depth of the wall penetration below the water surface. This modeling technique did not require any empiricism to describe the flow through the guard wall. The area under a guard wall controls the volume of flow through the wall.

VALIDATION: Model evaluations were made by comparing model results with laboratory data. Flume tests were conducted with the Type 5 design guard wall (365.76 m (1,200-ft) multicelled wall with a 9.14-m (30-ft) wall depth). Velocities at 0.6 depth resulting from a discharge of 3,546.68 cu m/sec (125,250 cfs) and a pool elevation of 12.80 m (42 ft) were measured at points

on a 7.62-m (25-ft) spacing across the navigation channel. The computed velocities were compared with the measured values at eight stations along the navigation channel as shown in Figure 1. The velocity distribution across the channel was plotted for each of the stations in Figures 2-9. The model accurately reproduced the velocities at locations upstream of the guard wall (Stations 4800, 2760, and 1920). However, the computed velocities were consistently less than those observed at the stations bounded by the guard wall (Stations 1265, 1015, 765, 515, and 265). This error suggested that the computed volume of flow under the guard wall was less than that in the physical model. This underprediction of flow under the guard wall was attributed to the use of the hydrostatic pressure assumption. The hydrostatic pressure model neglected the vertical accelerations as flow dived under the guard wall. Shallow water models underpredicted the flow rate under adverse pressure gradients (Berger and Stockstill 1994) such as those present near the wall.

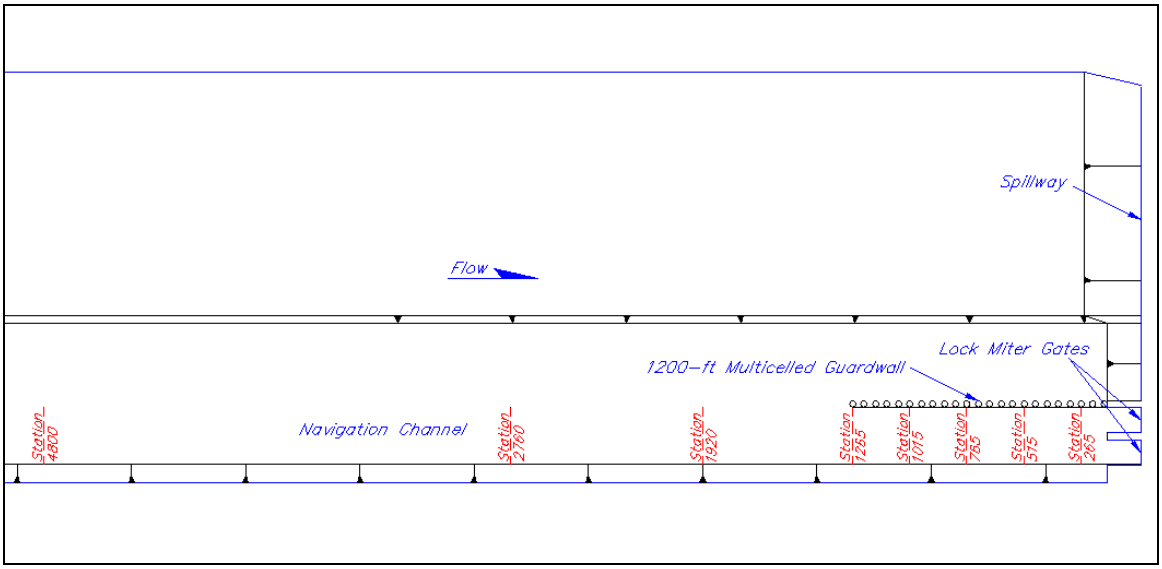

Figure 1. Location of stations along navigation channel

Adjustment of the wall draft would perhaps produce more accurate velocity predictions, but rather than developing rules pertaining to guard wall modeling, the research focused on computed flow fields relative from one design versus another. The numerical model will overpredict outdraft, but should serve as a practical tool for screening design ideas.

Although steady boundary conditions were specified, the wall configurations and adjacent spillway produced unsteady flow solutions. Eddies formed and shed from the end of the guard wall and an unstable eddy moved about within the area between the wall and the bank. The periods of these flow evolutions were design dependent. Therefore, comparisons between various designs required time averaging. The model results presented are time averages of 8-hr simulations.

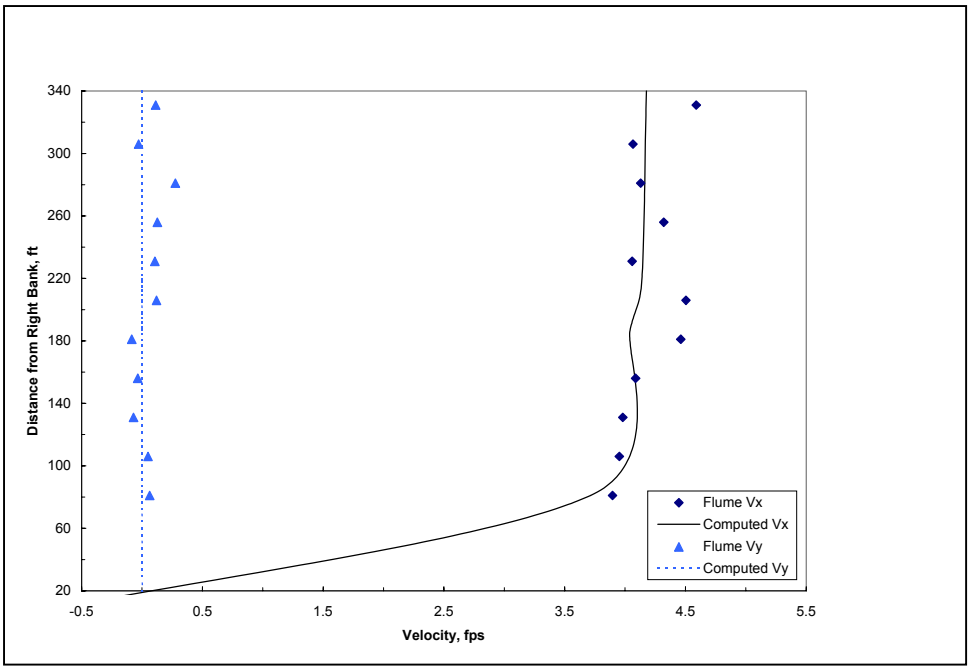

Figure 2. Velocity distribution across navigation channel, Sta 4800
(To convert feet per second to meters per second, multiply by 0.3048)

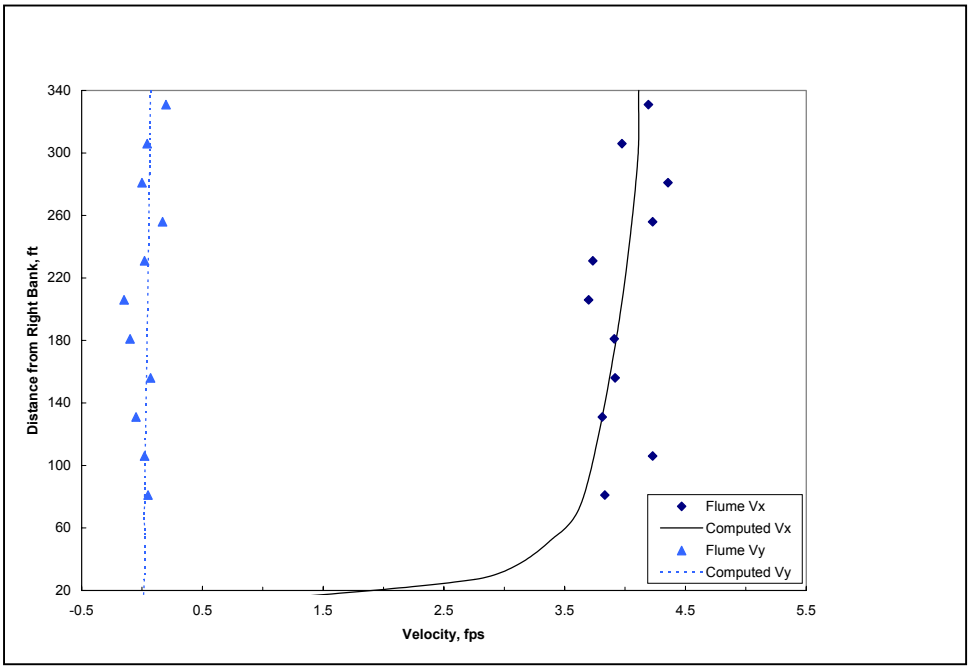

Figure 3. Velocity distribution across navigation channel, Sta 2760

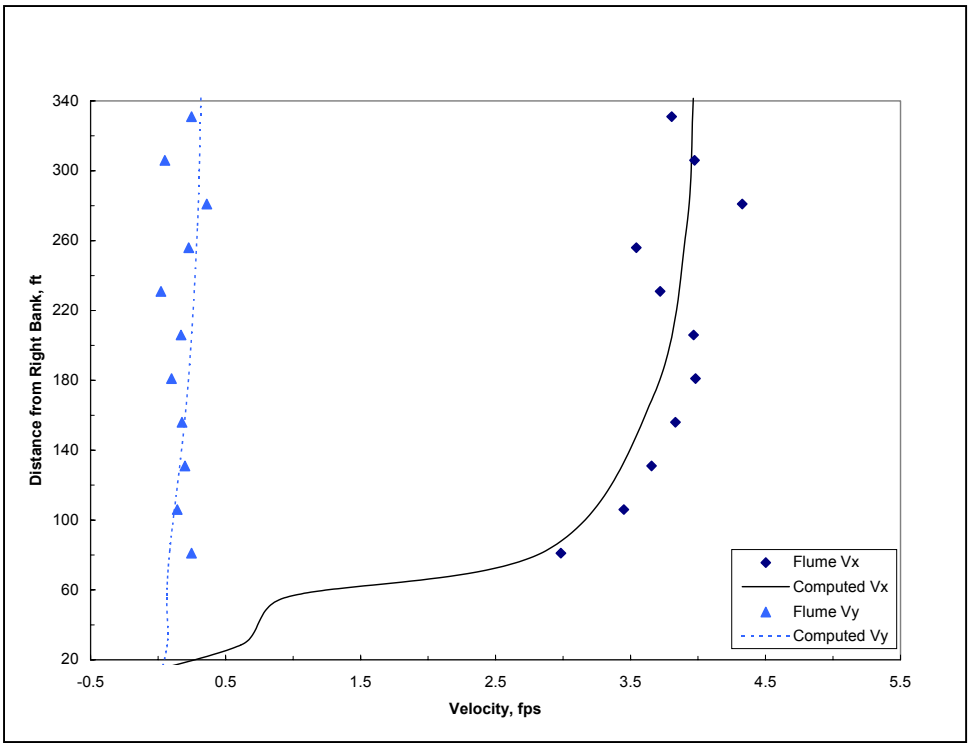

Figure 4. Velocity distribution across navigation channel, Sta 1920

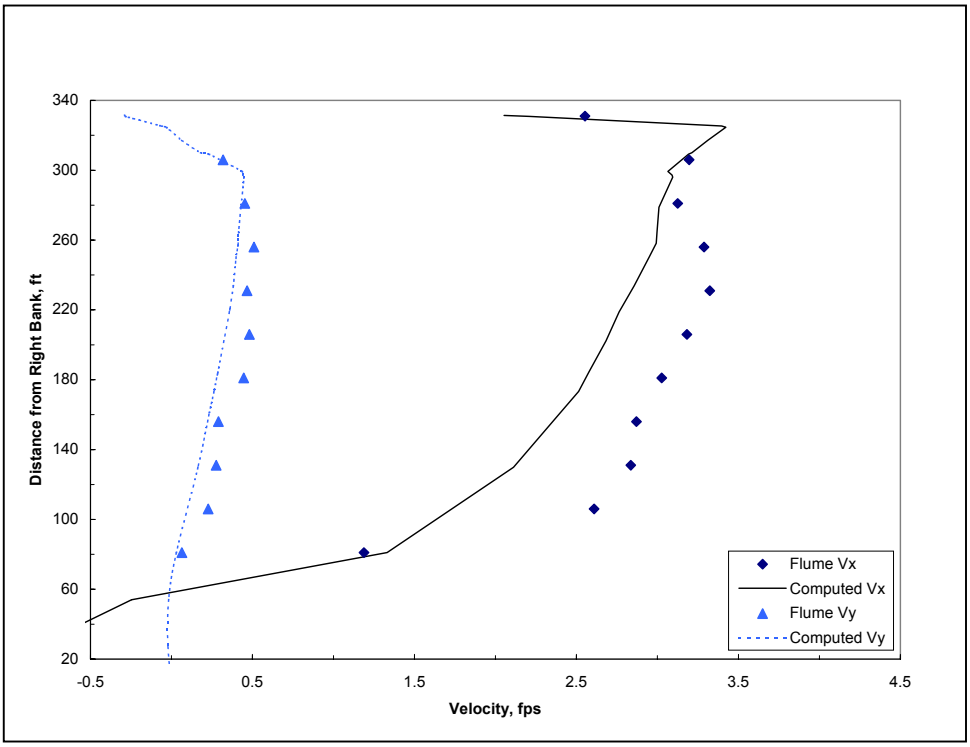

Figure 5. Velocity distribution across navigation channel, Sta 1265

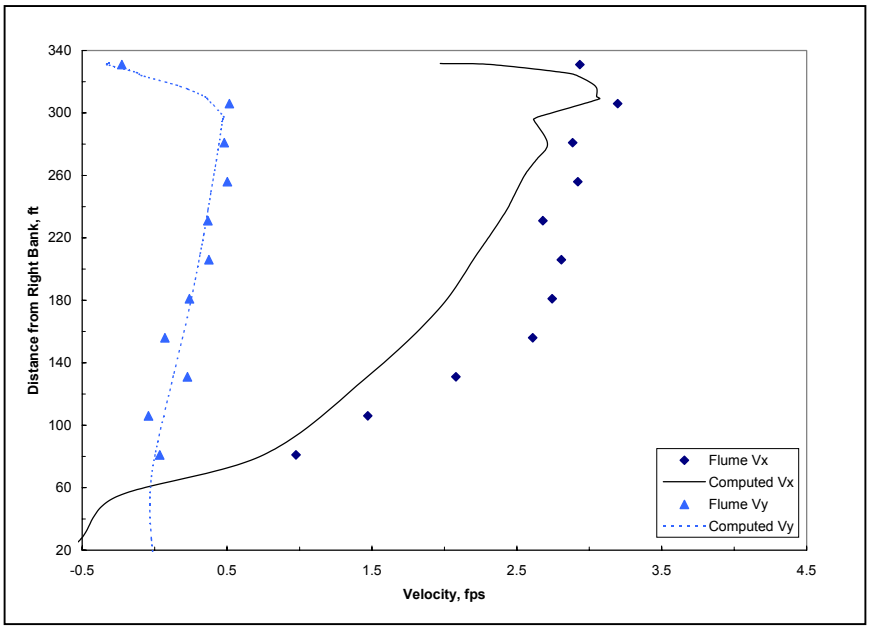

Figure 6. Velocity distribution across navigation channel, Sta 1015

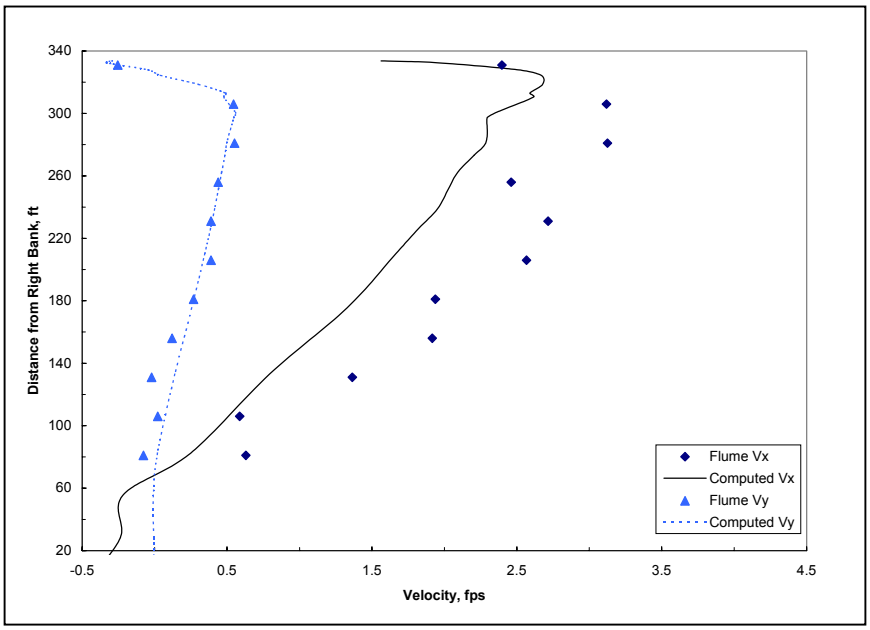

Figure 7. Velocity distribution across navigation channel, Sta 765

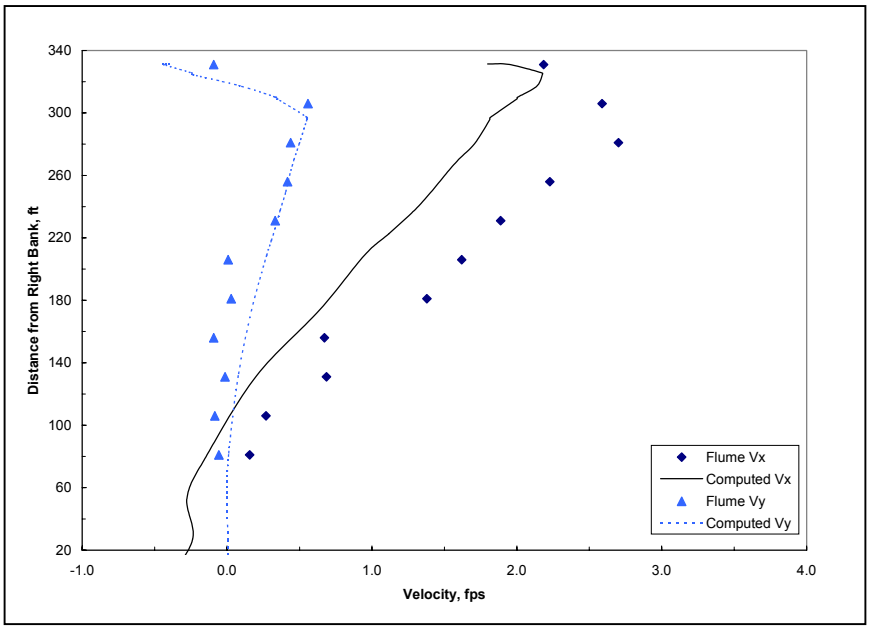

Figure 8. Velocity distribution across navigation channel, Sta 515

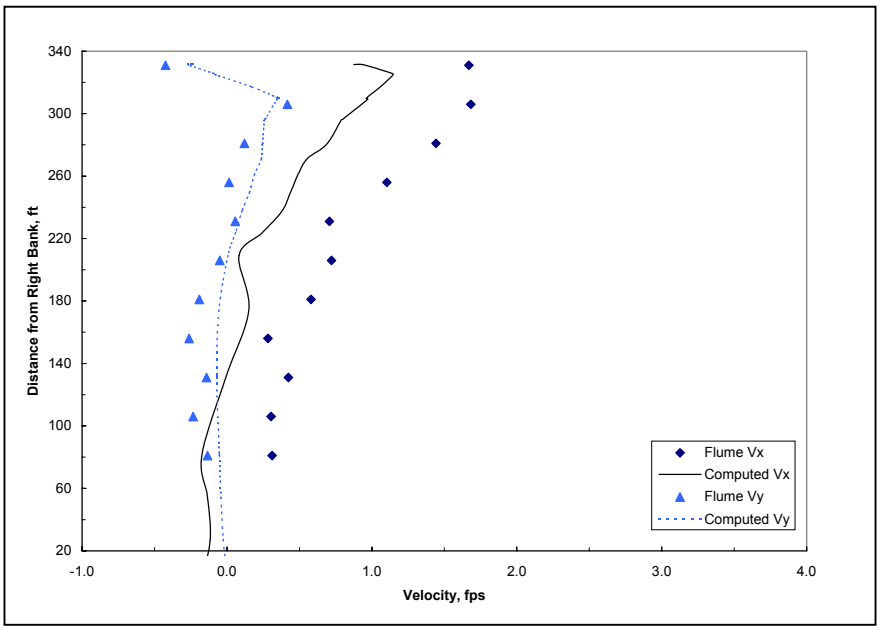

Figure 9. Velocity distribution across navigation channel, Sta 265

EVALUATING NAVIGATION CONDITIONS FROM MODEL RESULTS: These evaluations were intended to indicate the relative acceptability of various guard wall designs. The computed outdraft and draw toward the wall do not capture all of the forces acting on a tow, but rather serve as a means of ranking the designs on the basis of safe navigation conditions. Determination of the optimum navigation conditions is a balancing act between limiting outdraft, by providing more flow area under the wall, and limiting the draw toward the wall resulting from the under-wall flow. The draw toward the wall can cause the tow to strike the wall at an excessive speed and/or inhibit a tow resting on the wall from departing.

Navigation conditions were evaluated based on water-surface slopes in the approach. Outdraft was estimated from the lateral gradients in water surface without consideration of vessel effects. A 3-wide by 5-long barge train drafted at 2.74 m (9 ft) was used in all the calculations. The reported outdraft is the maximum lateral force exerted on a body having the barge train dimensions whose location was varied from 3.3 tow lengths upstream of the lock to the end of the guard wall and at various sailing lines within the navigation channel.

The draw toward the wall was determined for a 3 by 5 tow arrangement with the bow 0.2 tow lengths upstream of the lock and sitting 15.25 m (50 ft) (0.5 tow widths) away from the wall. Forces on the tow were approximated using the lateral water-surface gradients as was used in the outdraft calculations.

GUARD WALL DESIGN EVALUATIONS: Twenty-seven guard wall designs were evaluated using the numerical model to gain insight into the controlling features of guard walls. These designs included a solid wall, single multicell walls, and floating walls. A solid 365.76-m (1,200-ft) wall, 365.76-m (1,200-ft) and 274.32-m (900-ft) single multicell walls each having three different drafts, and 365.76-m (1,200-ft) and 274.32-m (900-ft) floating walls each having three different drafts were tested. Two approach widths, defined as the distance from the wall to the side-slope toe, were simulated for each configuration. A brief description of the designs is provided in Table 1.

Table 1
Guard Wall Configurations Modeled

Design	Approach width, m (ft)	Wall type	Wall length, m (ft)	el of bottom (curtain), m (ft)	Under-wall area-to-cross-section area ratio (Pool 42.0)
Type 2	76.2 (250)	Solid	365.76 (1,200)	NA	0.0
Type 3	76.2 (250)	Multicell	365.76 (1,200)	12.19 (40)	1.5
Type 4	76.2 (250)	Multicell	365.76 (1,200)	9.14 (30)	0.9
Type 5	76.2 (250)	Multicell	365.76 (1,200)	7.62 (25)	0.6
Type 6	76.2 (250)	Multicell	274.32 (900)	7.62 (25)	0.4
Type 7	76.2 (250)	Multicell	274.32 (900)	9.14 (30)	0.6
Type 8	76.2 (250)	Multicell	274.32 (900)	12.19 (40)	1.1
Type 9	76.2 (250)	Floating	365.76 (1,200)	12.19 (40)	3.3
Type 10	76.2 (250)	Floating	365.76 (1,200)	9.14 (30)	2.0
Type 11	76.2 (250)	Floating	365.76 (1,200)	7.62 (25)	1.3
Type 12	76.2 (250)	Floating	274.32 (900)	7.62 (25)	0.9
Type 13	76.2 (250)	Floating	274.32 (900)	9.14 (30)	1.4
Type 14	76.2 (250)	Floating	274.32 (900)	12.19 (40)	2.4
Type 15	76.2 (250)	Floating	365.76 (1,200)	6.09 (20)	0.7
Type 16	152.4 (500)	Multicell	365.76 (1,200)	12.19 (40)	0.8
Type 17	152.4 (500)	Multicell	365.76 (1,200)	9.14 (30)	0.5
Type 18	152.4 (500)	Multicell	365.76 (1,200)	7.62 (25)	0.3
Type 19	152.4 (500)	Floating	365.76 (1,200)	12.19 (40)	1.8
Type 20	152.4 (500)	Floating	365.76 (1,200)	9.14 (30)	1.1
Type 21	152.4 (500)	Floating	365.76 (1,200)	7.62 (25)	0.7
Type 22	152.4 (500)	Multicell	274.32 (900)	12.19 (40)	0.6
Type 23	152.4 (500)	Multicell	274.32 (900)	9.14 (30)	0.4
Type 24	152.4 (500)	Multicell	274.32 (900)	7.62 (25)	0.2
Type 25	152.4 (500)	Floating	274.32 (900)	12.19 (40)	1.3
Type 26	152.4 (500)	Floating	274.32 (900)	9.14 (30)	0.8
Type 27	152.4 (500)	Floating	274.32 (900)	7.62 (25)	0.5

The 365.76-m (1,200-ft) solid wall (Type 2 design) produced the flow field illustrated in Figure 10. The currents within the navigation channel upstream of the wall bend toward the main river. There is little flow between the land and the wall. A 365.76-m (1,200-ft) multicell wall (Type 5 design) allows flow under the wall as shown in the vector plot in Figure 11. A 365.76-m (1,200-ft) floating wall solution is shown in Figure 12. These solutions illustrate how sensitive the flow distribution is to the area provided beneath the guard wall.

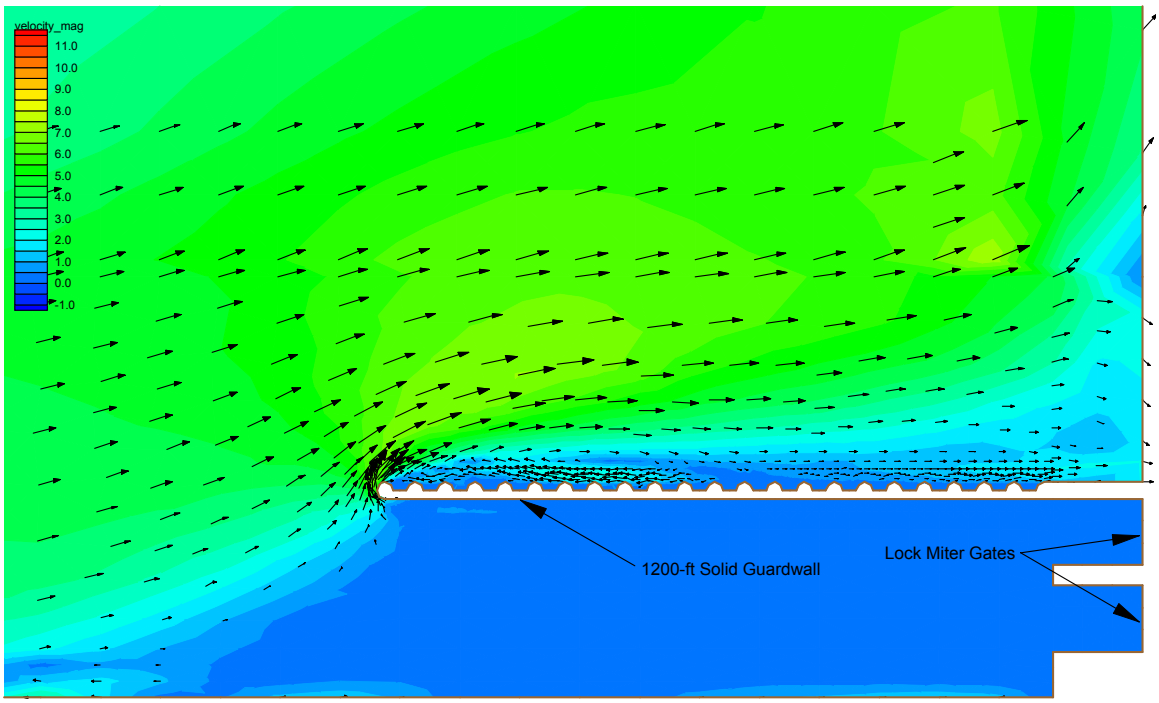

Figure 10. Type 2 design guard wall, 365.76-m (1,200-ft) solid wall, velocity vectors and contours

Three wall drafts were investigated. An extremely shallow wall (0.60-m (2-ft) draft), a wall having a curtain length of 3.65 m (12 ft) and one having a length of 5.18 m (17 ft) were investigated. A plot of flow distribution along the wall for various drafts (Figure 13) shows that as under-wall area-to-cross-sectional area decreases so that the flow control is at the under-wall area, the flow is more uniformly distributed along the wall. It is not suggested that uniform flow along the wall is required to have acceptable navigation conditions, but it does mean that flow concentrations that may accelerate the tow toward the wall are not present.

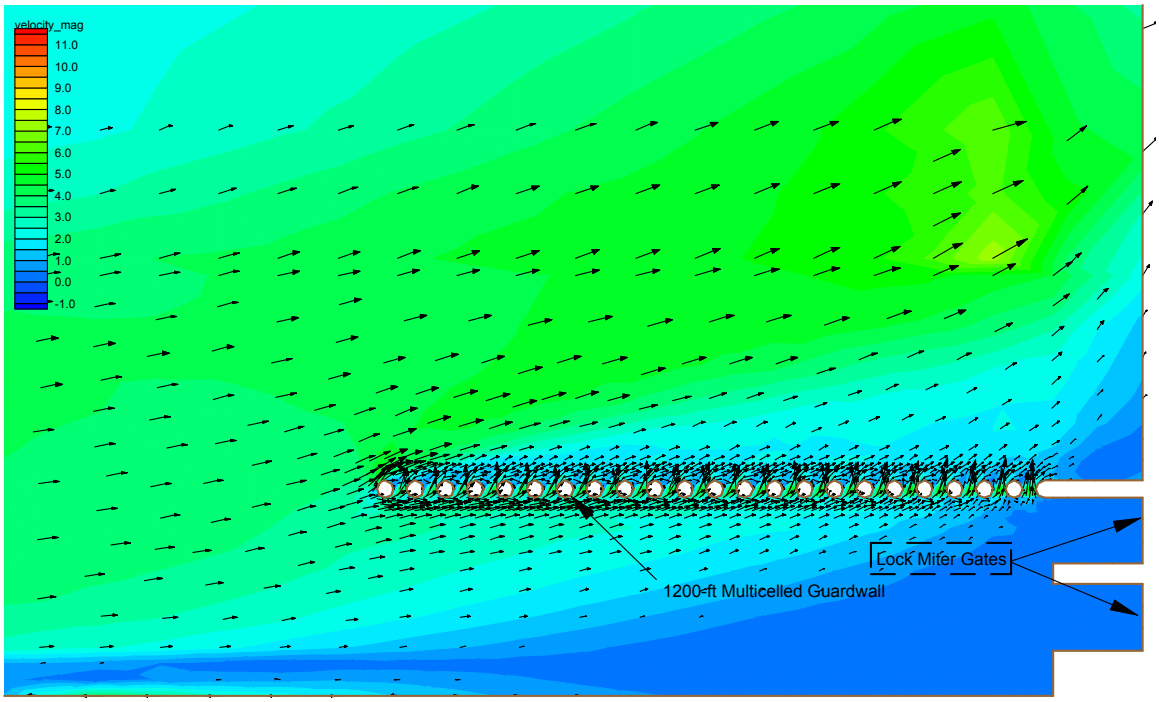

Figure 11. Type 5 design guard wall, 365.76-m (1,200-ft) multicelled wall, 9.14 m (30 ft) deep, velocity vectors and contours

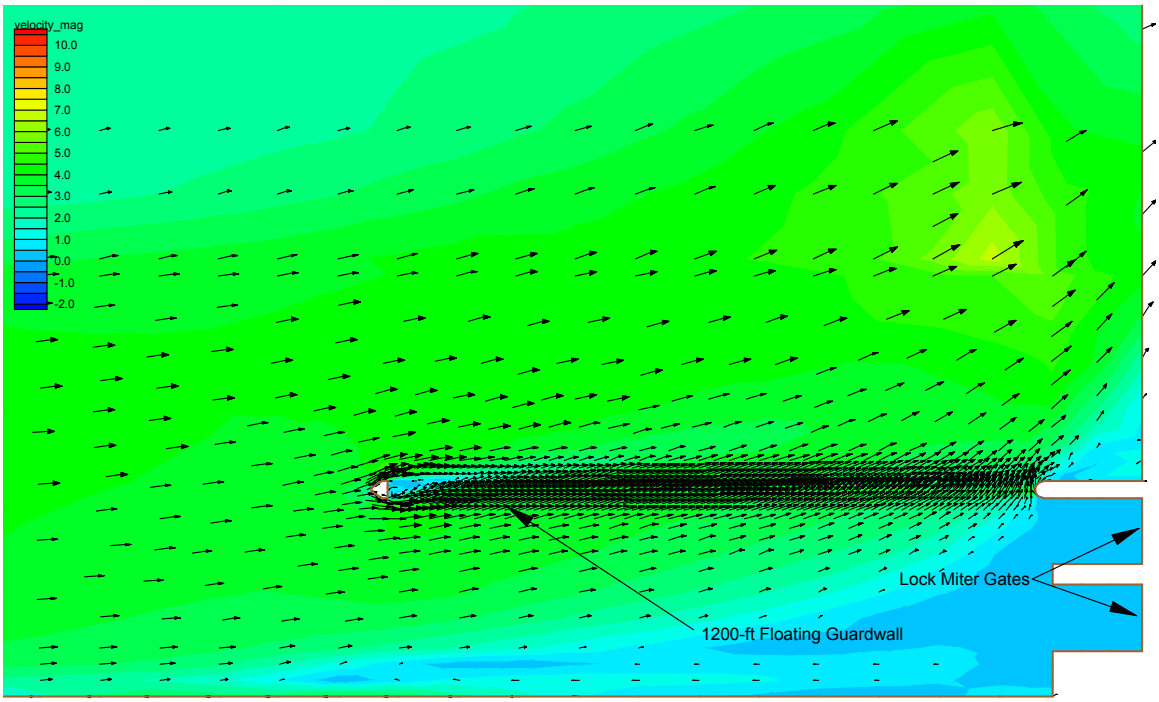

Figure 12. Type 10 design guard wall, 365.76-m (1,200-ft) floating wall, 9.14 m (30 ft) deep, velocity vectors and contours

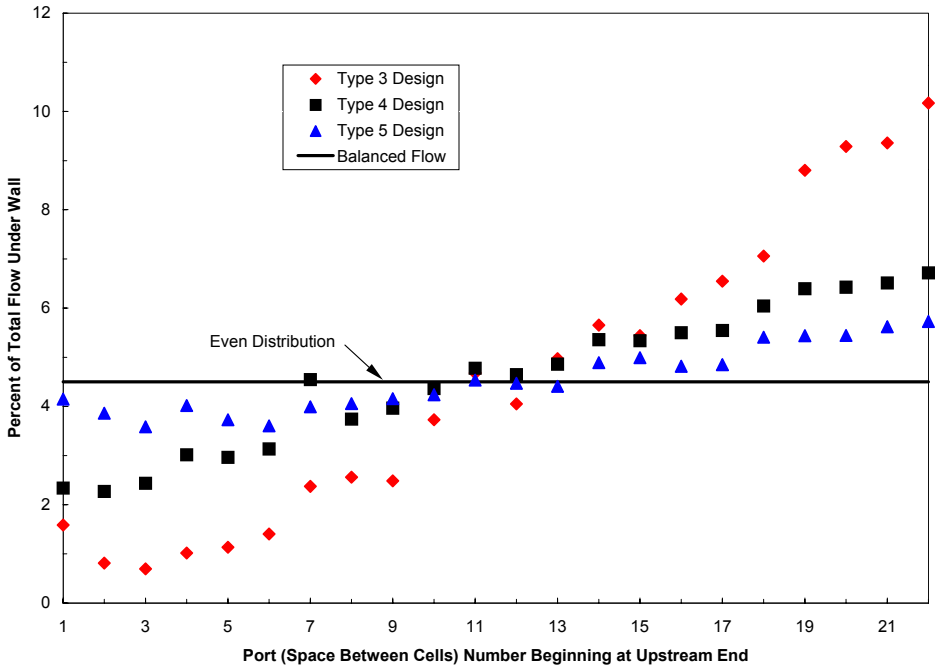

Figure 13. Flow distribution along multicelled wall

The estimated lateral forces are shown in the bar chart provided in Figure 14. The chart shows that designs such as the solid wall (Type 2) and others that have low under-wall flow area-to-cross-sectional areas (e.g., Type 24) produce large outdraft but negligible draw toward the wall. Larger forces were produced with wider approach width (152.4-m (500-ft), Types 16-27). Designs that have a very large port area such as the Type 3 design guard wall (365.76-m (1,200-ft) multicelled with 0.60-m (2-ft) draft) have very little outdraft, but extremely high draw toward the wall. This illustrates that an optimum guard wall design will have to balance outdraft and the draw toward the wall such as produced with the Type 4 design (best design evaluated).

The graph of forces as a function of wall flow area, shown in Figure 15, leads to the conclusion that designers should strive to have an area under the wall-to-cross-sectional area ratio of about 0.6.

ADDITIONAL INFORMATION: Questions about this CHETN can be addressed to Richard L. Stockstill (601-634-4251, e-mail: *Richard.L.Stockstill@erdc.usace.army.mil*). This Technical Note should be referenced as follows:

> Stockstill, R. L. (2001). "Modeling navigation conditions at lock approaches," Coastal and Hydraulics Engineering Technical Note CHETN-IX-6, U.S. Army Engineer Research and Development Center, Vicksburg, MS.
> *http://chl.wes.army.mil/library/publications/chetn/*

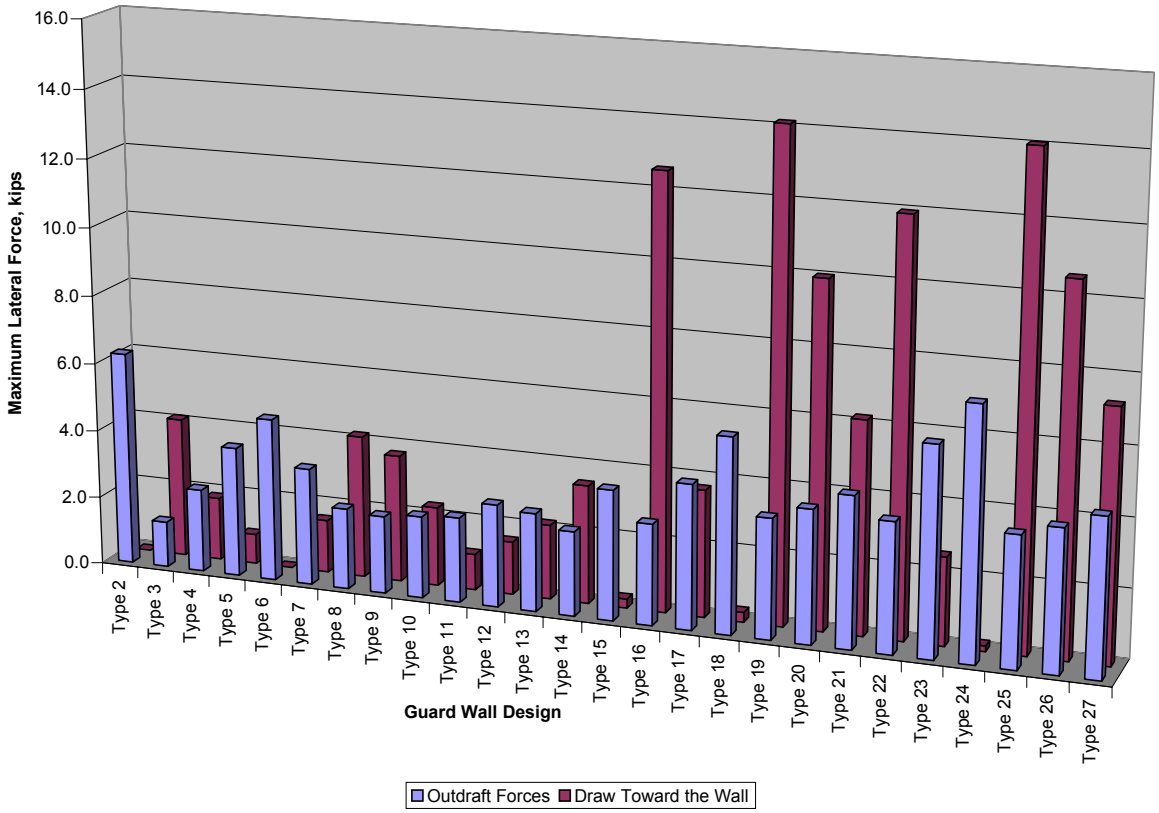

Figure 14. Comparisons of outdraft and draw toward the guard wall
(To convert kilopounds to newtons, multiply by 4,448.222)

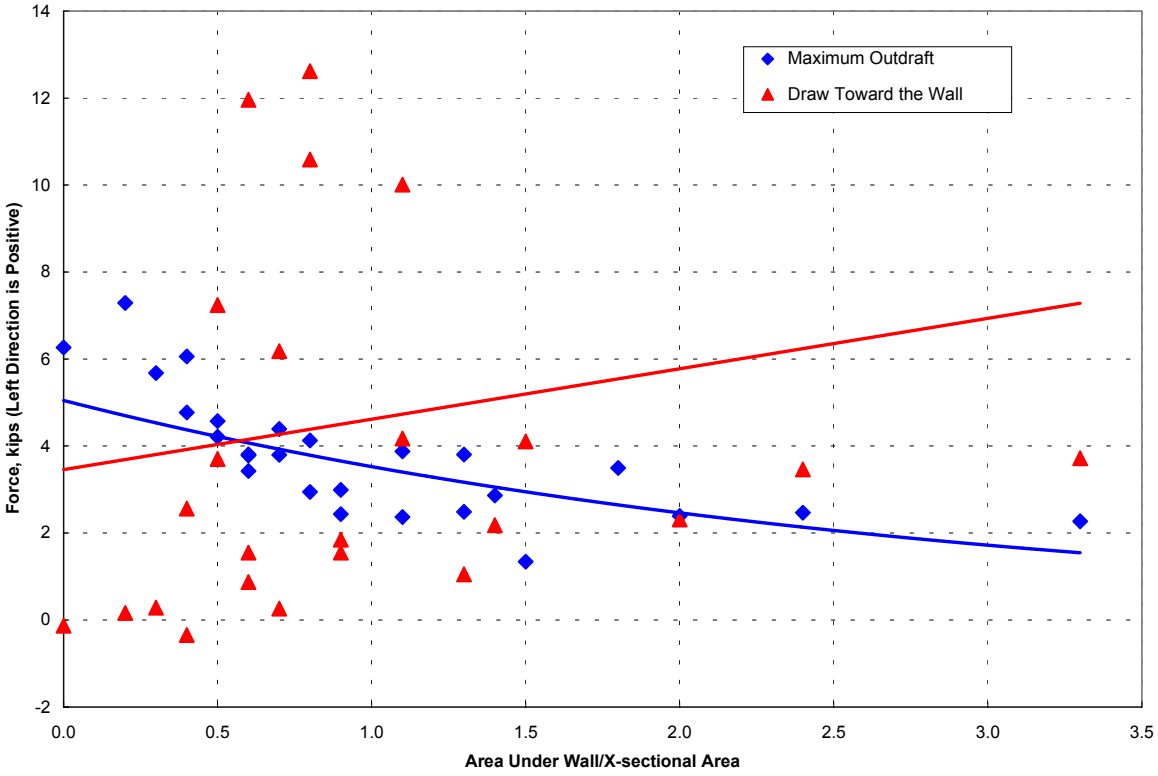

Figure 15. Effects of flow area under wall on outdraft and draw toward guard wall

REFERENCE

Berger, R. C., and Stockstill, R. L. (1994). "Considerations In 2-D modeling of hydraulically steep flow," Proc. 1994 National Hydraulics Conference, ASCE.